Some possible sources of IceCube TeV-PeV neutrino events

Sarira Sahu, Luis Salvador Miranda

Instituto de Ciencias Nucleares, Universidad Nacional Autónoma de México,

Circuito Exterior, C.U., A. Postal 70-543, 04510 Mexico DF, Mexico

arXiv:1408.3664v3 [astro-ph.HE] 31 Aug 2015

Abstract

The IceCube Collaboration has observed 37 neutrino events in the energy range $30\,TeV \leq E_\nu \leq 2$ PeV and the sources of these neutrinos are unknown. Here we have shown that positions of 12 high energy blazars and the position of the FR-I galaxy Centaurus A, coincide within the error circles of ten IceCube events, the later being in the error circle of the highest energy event so far observed by IceCube. Two of the above blazars are simultaneously within the error circles of the Telescope Array hotspot and one IceCube event. We found that the blazar H2356-309 is within the error circles of three IceCube events. We propose that photohadronic interaction of the Fermi accelerated high energy protons with the synchrotron/SSC background photons in the nuclear region of these high energy blazars and AGN are probably responsible for some of the observed IceCube events.

I. INTRODUCTION

In November 2012, the IceCube Collaboration announced the detection of two showerlike events with energies slightly above 1 PeV by analyzing the data taken during May 2010 - May 2012[1]. A follow-up analysis of the same data published in November 2013, revealed additional 26 events in the energy range $\sim$ 30 TeV - 250 TeV[2]. Reconstruction of these events shows that 21 events are showerlike, mostly caused by ν_e and ν_τ and 7 are muon track events. These 28 events have flavors, directions and energies inconsistent with those expected from the atmospheric muon and neutrino backgrounds and probably this is the first indication of extraterrestrial origin of high energy neutrinos. The track events have uncertainty of order one degree in their arrival directions and the angular resolution for 21 shower events is poor, ranging from$\sim 10^\circ$ to $\sim 50^\circ$. The IceCube analysis ruled out any spatial clustering of the events. The third year (2012-2013) data analysis revealed additional 9 events of which two are track events and rest are shower events [3]. The event 35 is the most energetic one so far observed. In the full 988-day data, the muon background is expected to be 8.4 ± 4.2 and the atmospheric neutrino is $6.6^{+5.9}_{-1.6}$. Five events are down going muons and are consistent with the expected background muon events. This shows that the IceCube events are predominantly shower events. For a E_ν^{-2} spectrum the best fit diffuse flux obtained by IceCube per flavor is $F_\nu = (0.95 \pm 0.3) \times 10^{-8}\, GeV\, cm^{-2}\, s^{-1}\, sr^{-1}$ which is consistent with the Waxman-Bahcall bound[4]. Observation of these neutrinos triggered a lot of excitement to understand their origin and production mechanism. While interpreting these events in terms of astrophysical models seems challenging, several possible galactic and extra galactic sources have been discussed which includes, Galactic center[5], γ-ray bursts (GRBs)[6], active galactic nuclei (AGN)[7], high energy peaked blazars (HBLs)[8, 9], starburst galaxies[10] etc. In Ref.[8] many positional correlations of BL Lac objects and galactic pulsar wind nebulae with the IceCube events are shown. It is also very natural to expect that these neutrinos might come from diverse sources having different production mechanisms and different power-law and this information can probably be extracted from the directionality of the observed neutrino events. The largest concentration of 7 events are around the Galactic center and also clustering of the events could be associated to the Norma arm of the Galaxy[11]. As the statistics is too sparse, it is premature to draw any conclusion regarding the galactic origin of these events. There are also nonstandard physics

interpretations of these events[12, 13].

We found coincidence of 12 TeV emitting HBL positions and the FR-I galaxy Centaurus A (Cen A) within the error circles of 10 IceCube events from the online catalog for TeV astronomy (TeVCat)[14]. cat. Due to the observed multi-TeV emission, these objects are long believed to be sources of ultra high energy cosmic rays (UHECRs). Few years ago, Pierre Auger (PA) collaboration reported two UHECR events within 3.1° around Cen A. Therefore, in this work we focus our analysis on these candidate sources to find out how the IceCube events with the desired energies can be produced through photohadronic interaction within the core region of the emanating jets.

II. HADRONIC MODEL

In the framework of the unification scheme of AGN, blazars and radio galaxies[15], all are intrinsically the same objects, viewed at different angles with respect to the jet axis. The blazars have jets pointing towards us. The double-peak spectral energy distribution (SED) structure is common to all these objects. This model is successful in explaining the multi-wavelength emission from BL Lac objects and FR-I galaxies[16–20]. However, multi-TeV emission during flaring and non-flaring events from these objects are difficult to reconcile. Also the most important challenge for the leptonic model is to explain the orphan flaring from the blazars 1ES1959+650 and Mrk 421. So variant of the hadronic models or the lepto-hadronic models are proposed to explain these multi-TeV emissions.

The AGNs are efficient accelerators of particles through shock or diffusive Fermi acceleration processes with a power-law spectrum given as $dN/dE \propto E^{-\kappa}$, with the power index $\kappa \geq 2$[21]. Protons can reach ultra high energy (UHE) through the above acceleration mechanisms. Fractions of these particles escaping from the source can constitute the UHECRs arriving on Earth. These objects also produce high energy γ-rays and neutrinos through pp and/or $p\gamma$ interactions [22]. The multi-TeV flaring events in blazars can be well explained by invoking hadronic model through $p\gamma$ interaction[23–25]. Here it is assumed that the multi-TeV flaring in blazar occurs within a compact and confined region with a comoving radius R'_f inside the blob of radius R'_b[23] (henceforth $'$ implies jet comoving frame). In the context of leptonic model, the SED of the HBLs (the synchrotron and the IC peaks) are fitted by taking into account different parameters (the blob radius R'_b, magnetic field B', Doppler fac-

tor δ, bulk Lorentz factor Γ etc.). For the present work, instead of discussing detail about the SED of the individual HBLs, we use these best fit parameters from the leptonic models which are shown in Table 1 and the references are given for these objects. As discussed earlier, in the inner region, the photon density $n'_{\gamma,f}$ is very high compared to the photon density n'_{γ} in the outer region. The UHE protons undergo photohadronic interaction with the seed photons in the inner region in the self-synchrotron Compton (SSC) regime through the intermediate Δ-resonance. In a normal blazar jet, however, the photohadronic process is not the efficient mechanism to produce multi-TeV γ-rays and neutrinos because n'_{γ} is low, which makes the optical depth $\tau_{p\gamma} \ll 1$. However, the assumption of the compact inner jet region overcome this problem. The pion production in $p\gamma$ collision through Δ-resonance is

$$p + \gamma \rightarrow \Delta^{+} \rightarrow \begin{cases} p\,\pi^{0}, & fraction\ 2/3 \\ n\,\pi^{+}, & fraction\ 1/3 \end{cases} . \tag{1}$$

The π^{+} and π^{0} will decay to GeV-TeV neutrinos and γ-rays respectively. The optical depth of the Δ-resonance process in the inner compact region is $\tau_{p\gamma} = n'_{\gamma,f}\sigma_{\Delta}R'_{f}$, where $n'_{\gamma,f}$ is not known. By assuming the Eddington luminosity is equally shared by the jet and the counter jet in the blazar, for a given comoving photon energy ϵ'_{γ} in the synchrotron/SSC regime we can get the upper limit on the photon density as $n'_{\gamma,f} \ll L_{Edd}/(8\pi R'^{2}_{f}\epsilon'_{\gamma})$. We can also compare the proton energy loss time scale $t'_{p\gamma} \simeq (0.5\, n'_{\gamma,f}\sigma_{\Delta})^{-1}$ and the dynamical time scale $t'_{d} = R'_{f}/c$ in this region to estimate $n'_{\gamma,f}$, so that the production of multi-TeV γ-rays and neutrinos take place. Not to have over production of neutrinos and γ-rays, we can assume a moderate efficiency (a few percents) by taking $\tau_{p\gamma} < 1$ which gives $n'_{\gamma,f} < (\sigma_{\Delta}R'_{f})^{-1}$. The kinematical condition for the production of Δ-resonance in the observer's frame is

$$E_{p}\epsilon_{\gamma} = 0.32\frac{\Gamma\delta}{(1+z)^{2}}GeV^{2}, \tag{2}$$

where E_p and ϵ_{γ} are the proton and the seed photon energies respectively. In the decay of the Δ-resonance to nucleon and pion, each pion carries ~ 0.2 of the proton energy and from the pion decay each neutrino and photon carries $1/4$ and $1/2$ of the pion energy respectively. So the individual neutrino and photon energies are respectively $E_{\nu} = E_{p}/20$ and $E_{\gamma} = E_{p}/10$. This gives

$$E_{\nu}\epsilon_{\gamma} = 0.016\frac{\Gamma\delta}{(1+z)^{2}}GeV^{2}. \tag{3}$$

In a HBL, ϵ_{γ} can be calculated from the given neutrino energy if Γ and δ are known.

Object (Dec,RA);z,δ	ID	$\frac{E_\nu}{TeV}$	$\frac{\epsilon_\gamma}{keV}$	$R'_{f,15}$	$R'_{b,15}$	$n'_{\gamma,f,10}$	$F_{\nu,-9}$	$\delta\chi^2$
RGBJ0152+017[26]	1	47.6	179.	0.9	1.5	2.2	2.41	0.24
(1.77,28.14);0.08,25								
H2356-309[27]	7	34.3	111.	0.5	3.4	4.0	2.38	0.66
(-30.62,358.79); 0.165, 18	10	97.2	39.					0.47
	21	30.2	125.					0.29
SHBLJ001355.9 [28]	21	30.2	45.	1.0	35.	2.0	2.41	0.13
(-18.89,3.46);0.095,10								
KUV00311-1938	21	30.2	-	-	-	-	-	0.05
(-19.35,8.39);-,-								
Mrk421 [20]	9	63.2	46.	3.0	7.0	0.7	2.43	0.61
(38.19,166.01); 0.031, 14								
1ES1011+496 [29]	9	63.2	69.	5.0	10.	0.4	2.36	0.94
(49.43,153.77);0.212,20								
PKS2005-489 [30]	12	104.	31.	5.0	400.	0.4	2.42	0.33
(-48.83,302.36);0.071,15	15	57.5	53.					0.25
PG1553+113 [31]	17	200.	50.	3.0	10.	0.7	2.29	0.59
(11.19,238.94);0.4,35								
Mrk180 [32]	31	42.5	34.	5.0	20.	0.4	2.43	0.18
(70.16,174.11);0.045,10								
1ES0502+675 [33]	31	42.5	35.	5.0	10.	0.4	2.31	0.66
(67.62,76.98);0.341,13								
RGBJ0710+591 [34]	31	42.5	267.	5.0	20.	0.4	2.39	0.77
(59.15,107.61);0.125,30								
1ES1312-423 [35]	35	2004.	0.32	5.0	240.	0.4	2.40	0.85
(-42.6,198.75);0.105,7.								
Cen A (FR-I) [39]	35	2004.	0.056	0 .6	3.0	3.3	2.45	0.73
(-43.01,201.36);.00183,1								

TABLE I. The objects HBLs/AGN are shown in first column which are in the error circles of the IceCube events ID (second column). Below each object we also put their coordinates, Declination and Right Ascension (Dec, RA) in degree, redshift (z) and the Doppler factor (δ). In the third and the fourth columns the observed neutrino energy E_ν/TeV and the corresponding seed photon

III. RESULTS

We found coincidence of the positions of 12 HBLs and one radio galaxy, Cen A within the error circles of 10 IceCube events. These HBLs and AGN are taken from the online catalog TeVCat[14] and are observed in multi-TeV γ-rays. However, the redshift, Lorentz factor and doppler factor of some of these HBLs are not yet known. So whichever HBL has known z, Γ, δ and SED and lies within the error circle of the IceCube event we calculate the seed photon energy ϵ_γ necessary to produce the desired neutrino energy E_ν through photohadronic interaction. The events 25 and 34 have very large errors $> 40^\circ$, so we neglect these two events from our analysis. For the calculation of $n'_{\gamma,f}$, first we estimate the radius of the inner blob R'_f, which will satisfy the restriction $R_s < R'_f < R'_b$, where $R_s = 2G_N M_{BH}/c^2$ is the Schwarzschild radius of the central black of mass M_{BH}. The R'_b is obtained from the leptonic model fit to the SED of the object. The values of R'_f and R'_b for the objects are shown in Table 1. We assume a very conservative 1% energy loss of the UHE protons in the inner blob on the dynamical time scale t'_d which corresponds to a optical depth of $\tau_{p\gamma} \sim 0.01$ and $n'_{\gamma,f} \sim 2 \times 10^{10}\, R'^{-1}_{f,15}\, cm^{-3}$. The proton in the inner jet region has maximum energy $E_{p,max} \sim 3 \times 10^{17} (B'_f/G) R'_{f,15}\, eV$, where B'_f is the comoving magnetic field, which is higher than the outer region. For all neutrino flavors α we assume a power-law spectrum of the form

$$J_{\nu_\alpha}(E_\nu) = A_{\nu_\alpha} \left(\frac{E_\nu}{100\, TeV} \right)^{-\kappa}, \tag{4}$$

and the neutrino flux can be given as

$$F_\nu = \sum_\alpha \int_{E_{\nu 1}(1+z)}^{E_{\nu 2}(1+z)} dE_\nu E_\nu J_{\nu_\alpha}(E_\nu). \tag{5}$$

The normalization factor A_{ν_α} is calculated by using the 988 days IceCube data[2]. The integration limit is from 25 TeV to 2.2 PeV[40] and κ is the spectral index. For the luminosity distance calculation we take the Hubble constant $H_0 = 69.6\, km\, s^{-1}\, Mpc^{-1}$, $\Omega_\Lambda = 0.714$ and $\Omega_m = 0.286$. All the 37 IceCube events with their individual error circles in equatorial coordinates are shown in the sky map in FIG. 1. The 12 HBLs and the Cen A are within the error circles of 10 IceCube events which are also shown in the sky map. In Table 1, we have summarized all the relevant parameters of these 13 objects. All the correlated IceCube events are shower events with sub-PeV energies and the event 35 which is the only PeV event with $E_\nu \simeq 2$ PeV. Except the HBL, KUV00311-1993[14], all other have their z, Γ and δ

measured/fitted and SEDs are calculated from the leptonic model. For most of the objects ϵ_γ lies between the synchrotron peak energy and the forward falling tail of synchrotron energy with the exception of RGBJ0192+017[26] and 1ES1011+496[29]. In these two HBLs ϵ_γ lies in the beginning of the SSC spectrum and the values are 179 keV and 69 keV respectively. The corresponding photon densities and the neutrino fluxes are shown in Table 1. Our estimate of $n'_{\gamma,f}$ is based on the assumption of 1% energy loss of the UHECR proton for all the HBLs/AGN. We observed that by varying κ between 2.2 and 3.08 we found a small variation is the neutrino flux. So here we fix its value to 2.2.

The HBL, H2356-309[27] is within the error circles of three IceCube events 7, 10 and 21 and their corresponding synchrotron energies, $n'_{\gamma,f}$ and neutrino flux are shown in Table 1. Another two HBLs, SHBLJ001355.9[28] and KUV00311-1938 are also within the error circle of the event 21 and SHBLJ001355.9 has the corresponding synchrotron energy $\epsilon_\gamma \simeq 45$ keV. The blazar PKS2005-489[30] is in the error circles of the events 12 and 15 and to produce these neutrino events the photon energy is in the range 30 keV-53 keV which is near the synchrotron peak and the corresponding proton energy is in the range $1.2\,PeV \leq E_p \leq 2.1\,PeV$. These two events are also spatially correlated with the Fermi bubble. The event 17 has a mean energy of 200 TeV is correlated with the HBL, PG1553+113[31] and is the farthest one in our list with a redshift of $z = 0.4$. The $n'_{\gamma,f}$ and neutrino fluxes for PKS2005-489 and PG1553+113 are shown in Table 1.

Very recently the Telescope Array (TA) observed an UHECR hotspot above 57 EeV in a region within 20° radius circle centered at RA= 146.7° and Dec. = 43.2° [36], the shaded closed counter in the sky map in FIG 1. This region correlates with three neutrino events 9, 26 and 31. We found three HBLs: Mrk 180, 1ES0502+675 and RGBJ0710+591 within the error circle of the IceCube event 31. Interestingly, positions of two blazars, Mrk 421[20] and 1ES1011+496[29] are also simultaneously within the error circle of the IceCube event 9 and within the TA hotspot[8, 37]. The required E_p and ϵ_γ for Mrk 421 are 1.3 PeV and 46 keV respectively. The photon density and F_ν are shown in Table 1. Similarly for 1ES1011+496 also we have shown the $n'_{\gamma,f}$ and F_ν in Table 1.

Cen A is the nearest active radio galaxy and long been proposed as the source of UHECRs. Few years ago Pierre Auger (PA) Collaboration reported two UHECR events above 57 EeV within 3.1° around Cen A[38]. Its position coincides within the error circle of the IceCube event 35 having the highest neutrino energy of 2 PeV so far observed by IceCube. In

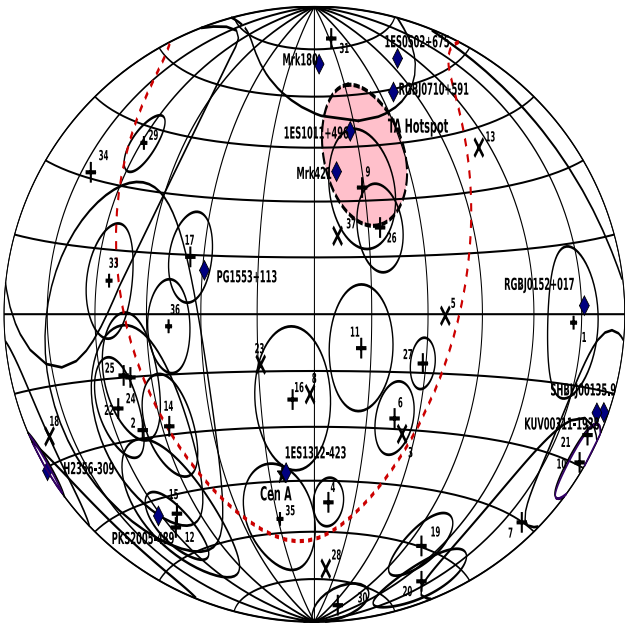

FIG. 1. The sky map is shown in the equatorial coordinates with the 37 IceCube events and their individual errors (only for shower events). Here + are shower events and × sign are track events with their corresponding event ID. We have also shown the positions of the HBLs with their names which are within the error circle of the IceCube events.The TA hotspot is shown as a shaded closed contour and the galactic plane is shown as a dashed line.

terms of the hadronic model discussed above the 2 PeV neutrino energy corresponds to a proton energy of ~ 40 PeV and the seed photons energy is $\epsilon_\gamma \sim 56$ eV in the valley formed by the synchrotron and the SSC photons. The seed photon density $n'_{\gamma,f} \sim \times 10^{10}\, cm^{-3}$ around $\epsilon_\gamma \sim 56$ eV is also high. For $\epsilon_\gamma < 56$ eV, synchrotron emission dominates and the low energy seed photon density increases rapidly[39]. So in principle $E_\nu > 2$ PeV can be produced more efficiently. But non-observation of neutrinos above 2 PeV from Cen A can be due to (i) low flux of UHECR above 40 PeV and/or (ii) there is a cut-off energy around 40 PeV beyond which the relativistic jet is unable to accelerate protons. Probably many more years of data are necessary to shed more light on this possible correlation between the IceCube event and the position of Cen A. Position of another HBL 1ES1312-423 also almost coincide with the position of the Cen A and thus falls within the error circle of the IceCube event 35. For this HBL the $\epsilon_\gamma = 0.32$ keV and the corresponding observed photon flux is $F_\gamma \sim 6 \times 10^{-12}\, erg\, cm^{-2}\, s^{-1}$ which is closed to the synchrotron peak[35].

The multi-TeV flaring of the objects 1ES1959+650, Mrk 421 and M87 are interpreted

through the photohadronic interaction as discussed in Section 2[23–25]. The maximum energy of these high energy γ-rays are less than 20 TeV (Mrk 421[25]) which corresponds to proton energy $E_p < 200$ TeV and neutrino energy $E_\nu < 10$ TeV. But for the interpretation of the IceCube events the necessary proton energy will be $E_p = 20 \times E_\nu$. For $30\,TeV \leq E_\nu \leq 2\,PeV$ the proton energy will be in the range $600\,TeV \leq E_p \leq 40\,PeV$. So neutrino flux from the interaction of these very high energy protons with the background photons can be small from an individual HBL. Apart from this, we have only observed flaring episodes of very few HBLs. So it is very hard to justify the temporal correlation of IceCube events during a flaring episode of a HBL. We have to wait longer period and have sufficient data to comment about the correlation between the IceCube events and the flaring episode of the object.

In the photohadronic scenario both the TeV-PeV neutrinos and the TeV-PeV γ-rays are correlated as both are produced from the decay of charged and neutral pions respectively as shown in Eq.(1). The background seed photons responsible for the production of these high energy neutrinos and γ-rays have energies above few keV. These photons have energy in between the synchrotron peak and the low energy tail of the SSC spectrum. The TeV-PeV photons produced from the π^0 decay will interact mostly with the same $\sim$ keV seed photons in the inner blob region to produce e^+e^- pairs. The required threshold energy for the seed photon to produce the pair is $\epsilon_{\gamma,th} \geq 2m_e^2/E_\gamma$ which is mostly in the microwave range. Also the $\sigma_{\gamma\gamma} \sim 1.7 \times 10^{-25}\,cm^{-2}$ is the maximum in the microwave range and the pair creation cross section for keV background photon is very small $\sigma_{\gamma\gamma} \leq 10^{-29}\,cm^2$. In the region where the TeV-PeV photons and neutrinos are produced, the microwave photon density is very low. So even if the seed photon density is high (in the keV range), the mean free path for the TeV-PeV photons satisfy $\lambda_{\gamma\gamma} \gg R'_f$, hence, there will be negligible attenuation of these photons in the inner blob region. Again in the outer blob, the low energy photon density is order of magnitude smaller than the inner blob, so no attenuation in the outer region. However, on their way to the Earth, these TeV-PeV photons can interact with the low energy photons to produce pairs.

We have also done a statistical analysis to look for the correlation between the IceCube events and the 42 TeV emitting HBL/AGN from the TeVCat[14]. Here we adopt the method

used in ref.[40] and convert the coordinates (RA and Dec) into unit vectors on a sphere as

$$\tilde{x} = (sin\theta\, cos\phi, sin\theta\, sin\phi, cos\theta), \tag{6}$$

with $\phi = RA$ and $\theta = \pi/2 - Dec$, where i and j correspond to the event coordinates and object coordinates respectively. The angle between the two unit vectors $\tilde{x}_i$ and $\tilde{x}_j$ is given as $\gamma = cos^{-1}(\tilde{x}_j.\tilde{x}_i)$ which is independent of the coordinate system and is a measure of correlation between the events and the objects. Then one makes use of the quantity

$$\delta\chi_i^2 = min_j \left(\gamma_{ij}^2/\delta\gamma_i^2\right) \tag{7}$$

where $\delta\gamma_i^2$ is the error on the ith coordinate. Only 10 events meet the condition that $\delta\chi^2 \leq 1$ with 13 objects which are shown in the sky map and also in Table 1. The $\delta\chi^2$ values of these events are given in the last column of Table 1. From the Monte Carlo simulation we estimate the significance of any correlation with IceCube events by randomizing the RA of the 42 objects within their allowed ranges. One has to remember that the value of $\delta\chi$ for the object closest to the neutrino event is chosen in this method. The distribution of $\delta\chi_i^2$ is realized by repeating this process one million times and the p-value is calculated by counting the number of times 10 or more IceCube events satisfy $\delta\chi^2 \leq 1$ divided by the total number of realizations. In Fig. 2, the shaded histograms correspond to the number of correlated neutrino events with the 42 objects of the TeVCat in different ranges of $\delta\chi^2$ value. The open histograms correspond to the expected number of correlated neutrino events from the simulations (continuous line for the randomized RA) with their corresponding p-value which is 0.647 corresponds to a confidence level (CL) of $\sim 35\%$. In another simulation we select the IceCube events which have angular errors $\leq 20^\circ$. In this case the IceCube events 7, 21 and 31 will not contribute. So with this constraint in angular resolution, we have only 7 events instead of 10 events considered earlier. In this simulation we found the CL $\sim 42\%$ this is shown in Fig. 3. Both of these analysis shows that there is no significant correlation between the IceCube events and the HBLs positions. As we have shown by increasing the angular resolution from 40° to 20° the CL increases by $\sim 7\%$. Also we believe that 42 objects from the TeVCat are not enough to give a better statistics when the events are isotropic. Apart from these objects there may be other type of sources which will contribute but are not included in our list. In future we would like to consider more sources for our analysis.

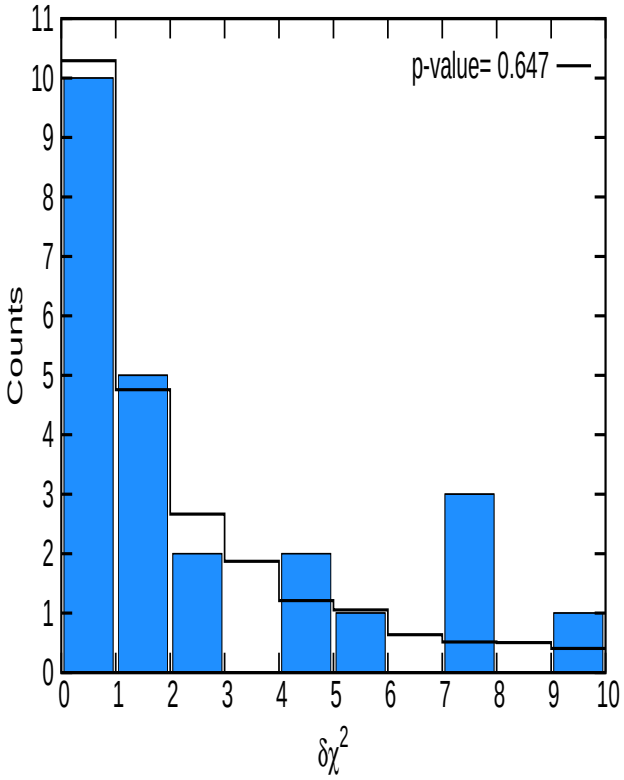

FIG. 2. The observed IceCube events (shaded histograms) and the simulated events (open histograms with continuous line is for random RA) for different $\delta\chi^2$ distribution are shown for angular resolution of the IceCube events $\leq 40^\circ$. The p-value for the open histograms are also given.

IV. CONCLUSIONS

The astrophysical interpretation of the 37 TeV-PeV neutrino events by IceCube is challenging and several viable candidates have been proposed and HBL is one of them. The HBLs are the sources capable of producing multi-TeV γ-rays. In the photohadronic scenario, TeV γ-rays are accompanied with multi-TeV neutrinos from the decay of charged pions and kaons. By analyzing the online catalog TeVCat[14] we found coincidence of 12 HBLs and one FR-I galaxy Cen A positions within the error circles of 10 IceCube events. All these events are found to be shower events. The position of the HBL, H2356-309 coincides with three IceCube events. We found positions of Mrk 421 and 1ES1011+496 are within the error circle of the IceCube event 9 as well as within the error circle of the TA hotspot. The observed highest energy PeV event coincides with the positions of Cen A and

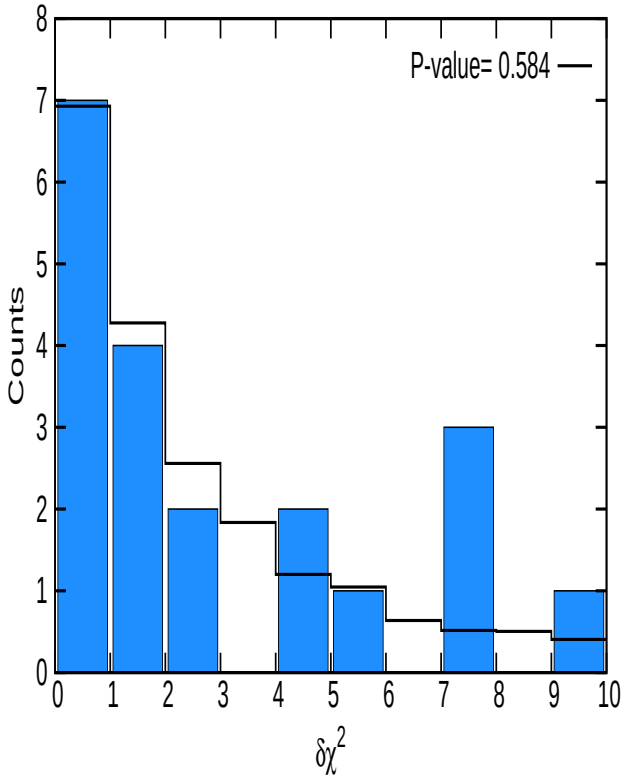

FIG. 3. Same as Fig. 2 but for angular resolution of the IceCube events $\leq 20^{\circ}$.

the the HBL 1ES1312-423. Although, from the statistical analysis we found no significant correlation between the IceCube events and the 42 objects in the TeV Catalog, it does not necessarily discard the photohadronic model interpretation for some of the IceCube events. Many more years of data are necessary to confirm or refute the positional correlations of the HBLs/AGN with the IceCube events. Also these possible candidate sources should be constantly monitored and studied in greater detail to have a better understanding of their properties and emission mechanisms.

We thank Paolo Padovani, Kohta Murase, Alberto Rosales de Leon, S. Mohanty, S. Razzaque and Lukas Nellen for many useful comments and discussions. The work of S. S. is partially supported by DGAPA-UNAM (Mexico) Projects No. IN103812 and IN110815.

[1] M. G. Aartsen *et al.* [IceCube Collaboration], Phys. Rev. Lett. **111**, 021103 (2013).

[2] M. G. Aartsen *et al.* [IceCube Collaboration], Science **342**, no. 6161, 1242856 (2013).

[3] M. G. Aartsen *et al.* [IceCube Collaboration], Phys. Rev. Lett. **113**, 101101 (2014).

[4] E. Waxman and J. N. Bahcall, Phys. Rev. D **59**, 023002 (1999).

[5] S. Razzaque, Phys. Rev. D **88**, 081302 (2013); M. Ahlers and K. Murase, Phys. Rev. D **90**, 023010 (2014); C. Lunardini, S. Razzaque, K. T. Theodoseau and L. Yang, Phys. Rev. D **90**, 023016 (2014); A. M. Taylor, S. Gabici and F. Aharonian, Phys. Rev. D **89**, 103003 (2014).

[6] K. Murase and K. Ioka, Phys. Rev. Lett. **111**, no. 12, 121102 (2013); K. Murase, K. Ioka, S. Nagataki and T. Nakamura, Astrophys. J. **651**, L5 (2006);

[7] K. Murase, Y. Inoue and C. D. Dermer, Phys. Rev. D **90**, no. 2, 023007 (2014); C. D. Dermer, K. Murase and Y. Inoue, JHEAp **3-4**, 29 (2014); W. Winter, Phys. Rev. D **88**, 083007 (2013); F. W. Stecker, Phys. Rev. D **88**, no. 4, 047301 (2013).

[8] P. Padovani and E. Resconi, Mon. Not. Roy. Astron. Soc. **443**, 474 (2014).

[9] F. Krauß, M. Kadler, K. Mannheim, R. Schulz, J. Trüstedt, J. Wilms, R. Ojha and E. Ros *et al.*, Astron. Astrophys. **566**, L7 (2014); F. Tavecchio, G. Ghisellini and D. Guetta, arXiv:1407.0907 [astro-ph.HE].

[10] K. Murase, M. Ahlers and B. C. Lacki, Phys. Rev. D **88**, no. 12, 121301 (2013); X. C. Chang and X. Y. Wang, Astrophys. J. **793**, no. 2, 131 (2014).

[11] A. Neronov, D. V. Semikoz and C. Tchernin, Phys. Rev. D **89**, 103002 (2014).

[12] C. Y. Chen, P. S. B. Dev and A. Soni, Phys. Rev. D **89**, 033012 (2014); K. Murase and J. F. Beacom, JCAP **1210**, 043 (2012); A. Esmaili and P. D. Serpico, JCAP **1311**, 054 (2013); A. Esmaili and Y. Farzan, JCAP **1212**, 014 (2012); P. Baerwald, M. Bustamante and W. Winter, JCAP **1210**, 020 (2012); S. Pakvasa, A. Joshipura and S. Mohanty, Phys. Rev. Lett. **110**, 171802 (2013).

[13] L. A. Anchordoqui, V. Barger, I. Cholis, H. Goldberg, D. Hooper, A. Kusenko, J. G. Learned and D. Marfatia *et al.*, Journal of High Energy Astrophysics **1-2**, 1 (2014).

[14] See the website: http://tevcat.uchicago.edu/.

[15] G. Ghisellini, A. Celotti, G. Fossati, L. Maraschi and A. Comastri, Mon. Not. Roy. Astron. Soc. **301**, 451 (1998); G. Fossati, L. Maraschi, A. Celotti, A. Comastri and G. Ghisellini, Mon. Not. Roy. Astron. Soc. **299**, 433 (1998); M. Chiaberge, A. Capetti and A. Celotti, Mon. Not. Roy. Astron. Soc. **324**, L33 (2001).

[16] G. Tagliaferri and L. Foschini, Astrophys. J. **679**, 1029 (2008).

[17] K. Gutierrez *et al.* [VERITAS Collaboration], Astrophys. J. **644**, 742 (2006).

[18] A. A. Abdo *et al.* [Fermi Collaboration], Astrophys. J. **719**, 1433 (2010).

[19] P. Roustazadeh and M. Bottcher, Astrophys. J. **728**, 134 (2011).

[20] M. Blazejowski, G. Blaylock, I. H. Bond, S. M. Bradbury, J. H. Buckley, D. A. Carter-Lewis, O. Celik and P. Cogan *et al.*, Astrophys. J. **630**, 130 (2005).

[21] C. D. Dermer and R. Schlickeiser, Astrophys. J. **416**, 458 (1993).

[22] M. Kachelriess, S. Ostapchenko and R. Tomas, New J. Phys. **11**, 065017 (2009); M. Honda, Astrophys. J. **706**, 1517 (2009).

[23] S. Sahu, A. F. O. Oliveros and J. C. Sanabria, Phys. Rev. D **87**, 103015 (2013).

[24] S. Sahu and E. Palacios, Eur. Phys. J. C **75**, no. 2, 52 (2015).

[25] S. Sahu, L. S. Miranda and S. Rajpoot, arXiv:1501.00973 [astro-ph.HE].

[26] F. Aharonian [HESS Collaboration], Astron. Astrophys. **481** , L103 (2008).

[27] F. Aharonian *et al.* [H.E.S.S. Collaboration], Astron. Astrophys. **455**, 461 (2006).

[28] A. Abramowski *et al.* [HESS Collaboration], Astron. Astrophys. **554**, A72 (2013).

[29] J. Albert *et al.* [MAGIC Collaboration], Astrophys. J. **667**, L21 (2007).

[30] A. Abramowski *et al.* [H.E.S.S. Collaboration], Astron. Astrophys. **533**, A110 (2011).

[31] J. Aleksic *et al.* [MAGIC Collaboration], Astrophys. J. **748**, 46 (2012).

[32] L. Costamante and G. Ghisellini, Astron. Astrophys. **384**, 56 (2002) [astro-ph/0112201].

[33] K. Katarzynski, Astron. Astrophys. **537**, A47 (2012) [arXiv:1110.5993 [astro-ph.CO]].

[34] V. A. Acciari, E. Aliu, T. Arlen, T. Aune, M. Bautista, M. Beilicke, W. Benbow and M. Bottcher *et al.*, Astrophys. J. **715**, L49 (2010) [arXiv:1005.0041 [astro-ph.HE]].

[35] A. Abramowski *et al.* [HESS Collaboration], arXiv:1306.3186 [astro-ph.HE].

[36] R. U. Abbasi *et al.* [Telescope Array Collaboration], Astrophys. J. **790**, L21 (2014).

[37] K. Fang, T. Fujii, T. Linden and A. V. Olinto, Astrophys. J. **794**, 126 (2014).

[38] The Pierre Auger Collaboration, Science **318**, 938 (2007).

[39] S. Sahu, B. Zhang and N. Fraija, Phys. Rev. D **85**, 043012 (2012).

[40] R. Moharana and S. Razzaque, arXiv:1501.05158 [astro-ph.HE].